SM13C-2514

CLUSTER CLOSE SEPARATION AT THE BOW SHOCK CAMPAIGN: INITIAL RESULTS.

Michael A. Balikhin[1], Roald Sagdeev[2], Simon N. Walker[1], Mikhail Malkov[3], Vladimir Krasnoselskikh[4], Yuri Khotyaintsev[5] Andrew Fazakerley[6], Natasha Doss[6]

[1]ACSE, University of Sheffield, Sheffield, UK; [2] University of Maryland, College Park, USA; [3] University of California, San Diego, USA; [4] LPCE CNRS, France; [5] IRF Uppsala, Sweden; [6] University College London, UK

ABSTRACT

The Cluster close separation campaign at the terrestrial bow shock was aimed at probing the terrestrial bow shock front using multi-scale spacecraft separations. The closest separation (< 10 km) was achieved between Cluster 3 and Cluster 4. The separation of two other spacecraft from this pair was in the range 100-1000 km. The data from this Cluster campaign have been used to study the fine structure of the magnetic ramp. It is shown that the magnetic field perturbations observed within the ramp along the shock normal possess spatial scales a few times shorter than the ramp region itself, and are accompanied by variations in the electric field with magnitudes of a few tens mV/m. Using dual spacecraft measurements enables us to show that in the plane of the shock front the characteristic width of these structures corresponds to electron scales. Comparison of the magnetic field profile obtained from Cluster 3 and 4 indicates possibility that the initial stage of the front reformation is observed.

INTRODUCTION

In spite of the great progress in the physics of the collisionless shocks that has been achieved since the pioneering theoretical development of the collisionless shock concept (e.g. Sagdeev 1961) a few unsolved problems still remain. One of them is the non-stationarity of high Mach number shocks. An understanding of shock front non-stationarity provides an insight into the physical processes that are involved in the formation of high Mach number shocks. The importance of shock front non-stationarity is also related to the fine structure of the front resulting from various scenarios of the non-stationarity. For example the model of magnetic ramp dynamics proposed by Krasnosel'skikh, (1985) leads to the occurrence of strong, localized electric field structures that can significantly affect the process of the electron thermalization within the shock front. To address this unsolved problem the ESA Cluster mission conducted a special Small Scale Campaign aimed at the observation of terrestrial bow shock with very small (only a few km) satellite separation distances. Here the initial results of this Cluster shock campaign relevant to the shock nonstationarity are presented.

Bow Shock crossing by Cluster on the 24th of January, 2015 at 21:10 UT.

Figure 1 shows the magnitude of the magnetic field |B| as measured by four Cluster spacecraft during the terrestrial bow shock crossing on 24th January 2015.

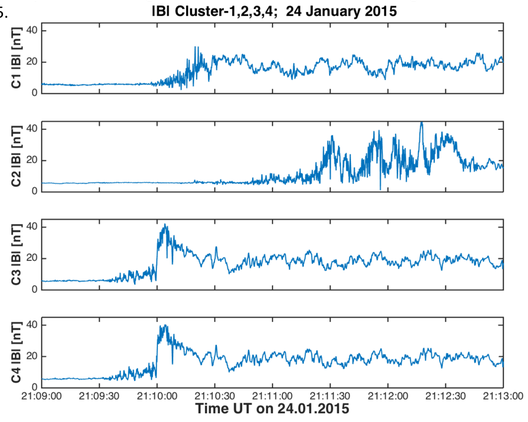

Figure 1. |B| as measured by four Cluster spacecraft during the shock crossing

During this shock crossing the closest separation of only 6.76 km was between Cluster 3 and 4. The separation distances between the Cluster 3 and Cluster 1,2 were 4002km and 3076km respectively. Initially the spacecraft were in the undisturbed solar wind with $|B_0|\approx 5.8$ nT. However, between 21:09:30 and 21:13:00 all spacecraft crossed the shock and entered the magnetosheath. Cluster 3 and 4 observed the shock ramp almost simultaneously, just after 21:09:59. As can be seen from Fig. 1 upstream of the ramp at 21:09:35-21:09:59 Cluster 3,4 observed the foot, evident from the gradual increase in |B|. The Peredo et al., (1995) model was used to calculate the shock normal n=[0.97668 0.20947 0.04700] (GSE). θ_{Bn} resulting from this normal is 66° and the Alfven Mach number $M_A\approx 7.8$. The separation between Cluster 3 and 4 along the model normal was ≈4.72km and ≈4.84 km in the perpendicular plane. Figure 2 displays the components of the magnetic field as measured by Cluster 3 in the shock coordinate system. The absence of significant variations in B_n during the ramp crossing supports the choice of the normal direction. The main change within the ramp occurs in B_l as expected.

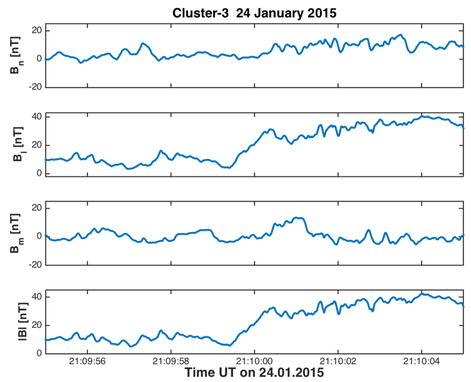

Figure 2. Three components of the magnetic field as measured by Cluster-3

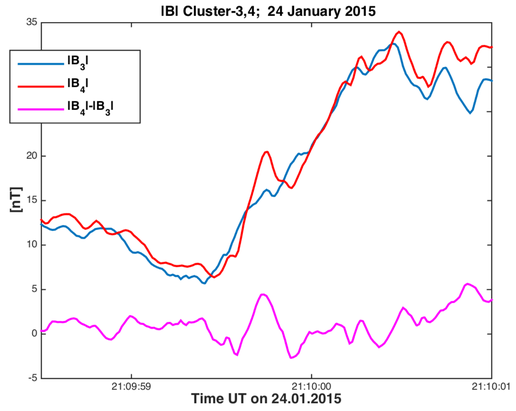

Figure 3.

Figure 3 displays |B| observed by Cluster 3 (blue) and 4 (red) using an expanded time scale. The main dissimilarity in |B| is the prominent local field maximum observed by Cluster 4 within the ramp. Such non-monotonic features have been observed before [Balikhin et al., 2005, Walker et al., 1999], however in the absence of close simultaneous measurements they also could be explained by a short lived reversal of the shock-spacecraft velocity during the ramp crossing. The close separation between C3 and C4 (of the order of the electron inertial scale) and simultaneous observation of the ramp by both spacecraft prove that the observed feature is a sub-structure of the ramp, and cannot be explained by a velocity reversal. The magenta line represents the difference $|B_4|-|B_3|$, and displays a clear oscillation at the time of the local maximum in the ramp magnetic field detected by Cluster 4. This oscillation is also evident in the difference of the magnetic field components B_l and B_m as measured by Cluster 4 and 3. The minimum variance direction for this oscillation (which corresponds to the direction of wave vector) forms a small angle 7° with the shock normal, and exhibits elliptical polarization as shown in Figure 4 that displays the relations between maximum, intermediate and minimum variance components. The red stars identify the initial part of the time interval.

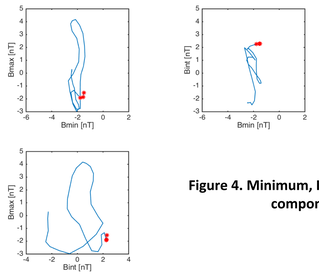

Figure 4. Minimum, Intermediate and Maximum components Variance

Currently, only limited electric field data are available from Cluster due to the failure of a number of electric field probes during 15 years of operation. Electric field data are not available on Cluster 3 and only Y-component of the electric field in the spacecraft non-spinning coordinate frame is reliably available from Cluster 4 for this bow shock crossing. The spacecraft y-axis is close to the y-axis in the GSE coordinate frame. The variation of E_y and |B| are shown in Figure 5. It can be seen that immediately after the local maximum of |B| within the ramp structure the increased level of E_y variations. To calculate the cross-shock potential Φ the projection of the electric field along the shock normal should be integrated along the normal direction. Assuming that V_{sh} is constant:

$$\Phi = \int_{t_o}^{t} E_n(\tau) V_{sh} d\tau$$

With only one reliably available component of the electric field it is impossible to calculate E_n and therefore Φ. With only one component available some very strong assumptions that are difficult to justify are needed to estimate Φ. One possibility is to assume that E_y is proportional to E_n. As the angle between the GSE y axis and the model shock normal is 78°, only a tiny part of E_y contributes to the cross shock potential. However the overall value of the potential can be estimated using results of statistical studies of the potential as a function of θ_{Bn} and M_A [Dimmock et al., 2012].

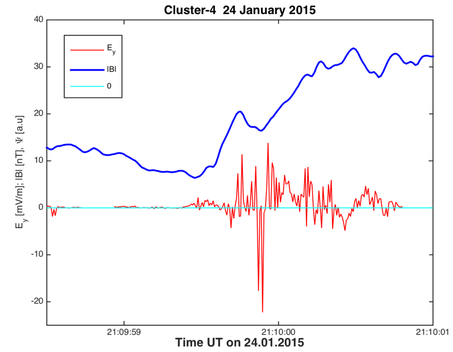

Figure 5. |B| and E_y as measured by Cluster 4.

Shock-Spacecraft Velocity and ramp spatial scales

For this particular shock crossing the determination the relative shock-spacecraft velocity V_{sh} is a challenging task. The separation between Cluster 4 and Cluster 1,2 forms angles 87.4° and 89.5° with the model shock normal. Separation between Cluster 3 and 4 is very small, implying a large error if this pair is used for the velocity identification, even though the angle with the shock normal is 45.8° The separation between Cluster 1 and 2 is about 3688km and forms angle 78.7° with the model shock normal. With all these reservations V_{sh} has been estimated using time delays between the following pairs: (1,4) and (1,2) resulting in the values 9.5km/s and 9.2km/s. Another possibility is to use a methodology from the "pre-ISEE" era that is based on the width of the foot region (Woods, 1969; Livesey et al., 1984):

$$L_{foot} \approx 0.68 \frac{V_{SW}}{\Omega_{ci}} \sin(\theta_{Bn})$$

Taking into account the upstream solar wind velocity and the foot duration leads to an estimate $V_{sh}\approx 14$km/s, that is surprisingly close to the above estimates based on the time delays in spite of the unfavorable geometry. It is the value of the velocity that based on the foot duration that is going to be used for the estimate of the shock ramp spatial scales. The duration of the ramp crossing is about 1 second corresponding to width of $L_{ramp}\approx 14$ km.

The characteristic spatial scales for this crossing are the following: electron inertial length $c/\omega_{pe}\approx 1.6$ km; ion inertial length $c/\omega_{pi}\approx 68.7$ km; dispersion length $\cos(\theta_{Bn})c/\omega_{pi}\approx 27.9$ km. Therefore $L_{ramp}\approx 8.75c/\omega_{pe}\approx 0.5\cos(\theta_{Bn})c/\omega_{pi}$.

The duration of the sub-structure within the ramp that corresponds to the local maximum observed in |B| is about 0.24 s, corresponding to the spatial scale along the normal $L_{n\text{-}sub}\approx$ 3.4 km$\approx 2.1c/\omega_{pe}\approx 0.12\cos(\theta_{Bn})c/\omega_{pi}$. The upper limit on the spatial scale of the substructure in the plane perpendicular to the normal can be estimated using the component of the Cluster 3 and 4 separation vector that is perpendicular to the normal, as this substructure is prominent in Cluster 4 data and is not clear in Cluster 3 data. Therefore: $S_{perpsub} \le 4.8$ km$\approx 3c/\omega_{pe}\approx 0.17\cos(\theta_{Bn})c/\omega_{pi}$.

Discussion

One of the explanations for substructures in the ramp, such as the local maximum observed by Cluster 4 and shown in Fig. 3, is shock front rippling. However the spatial scales associated with the corrugation instability that is known to lead to shock rippling are much larger than those observed here and correspond to MHD or at least ion scales.

Numerical simulations by Quest (1985; 1986) of high Mach number (22) perpendicular shocks exhibited quasi-periodic behavior in the ion reflection process. There were periods when all ions were reflected from the shock front were intermixed with periods without any reflection ions. Vaisberg et al., (1986) reported oscillations of the ion flux at the shock front. The quasi-periodic dynamics of the reflected ions must be related to the quasi periodic reformation of the macroscopic fields in the shock front. The analytical model for the non-stationary evolution of high Mach number shocks has been developed by Krasnoselskikh (1986) and Galeev et al., (1986) and reviewed in Krasnoselskikh et al. (2002). The Krasnoselskikh et al., model is based on the results of Sagdeev (1966), describing the relationship between the shock front structure and the corresponding linear waves. In brief, the Krasnoselskikh et al (2002) model assumes that for low Mach number dispersive shocks steepening of the front will stop once the front scale reaches the whistler dispersion scale. At this stage a phase standing precursor will be formed in a quasiperpendicular shock. This whistler precursor decelerates the upstream flow and provides the dissipation for example via the parametric instability. However, phase standing whistlers can exist only if the Mach number is below the whistler critical Mach number (M_w) (μ is the electron to proton mass ratio): $M_W = \frac{|\cos\theta_{Bn}|}{2\mu^{1/2}}$

If $M_A > M_W$ a stationary precursor can not be formed. The ramp steepening continues, and nonlinear whistler waves with a characteristic spatial scale c/ω_{pe} are formed within the ramp. The electric field related to this short scale nonlinear structure can lead to non adiabatic heating of electrons at the ramp [Balikhin et al., 1993]. If the Mach number exceeds $M_{nW}\approx 2^{1/2}M_W$ there is no possibility that these nonlinear waves will be generated within the ramp and the gradient catastrophe regime develops with quasi-periodic breaking of the shock front, similar to the breaking of large amplitude ordinary hydrodynamic waves. For the shock presented here $M_W\approx 8.7$, and $M_{nW}\approx 12.3$. Therefore the shock is very close the regime between these two critical Mach numbers. Cluster 4 observes oscillations that were predicted by Krasnoselskikh (1985).

Another scenario resulting in nonstationarity of the front, often referred to as front reformation, is evident in many numerical simulations (e.g. Krasnoselskikh et al., 2002). In this scenario the leading small amplitude whistler wave at the upstream edge of the foot grows to form a new ramp. It was shown in Krasnoselskikh et al , (2013) that this may be an artifact of the set of parameters used in simulations. In their attempt to reproduce the shock features reported by Lobzin et al. (2007), Comisel et al. (2011) used a ID PIC simulation with a realistic ion to electron mass ratio. The only unrealistic parameter in the simulation was the ratio of the electron plasma and cyclotron frequencies (ω_{pe}/Ω_{ce}). While agreeing that the shock was non-stationary, the results showed a number of substantial differences between simulation and observations. The electric fields in the vicinity of the shock front were much larger in the simulation than in the observations. The reason for this difference arises due to the use of an unrealistic value for ω_{pe}/Ω_{ce}. The refractive index (N) of the waves determines the ratio of the wave electric and magnetic fields and may be calculated from the phase velocity of the waves and, importantly, is related to the ratio ω_{pe}/Ω_{ce}.

$$N = \frac{kc}{\omega} = \frac{c}{V_{ph}} = \frac{cB}{E_{kperp}} = \frac{c}{M_A V_A} = \frac{\omega_{pi}}{M_A \Omega_{ci}} = \frac{\omega_{pe}}{M_A \Omega_{ce}} \frac{1}{\sqrt{\mu}}$$

For a phase standing whistler wave just upstream of the ramp the phase velocity is approximately the same as the upstream solar wind velocity. Observations showed that V_{sw}~440 kms^{-1}, resulting in N_{exp} ~ 700. However, for the simulation the value of ω_{pe}/Ω_{ce} was assumed to be 8 and hence N_{sim} ~ 23. Thus the electric field of the waves in the simulation was approximately 30 times greater than that observed. This significantly overestimated electric field can have an essential effects on the upstream ion dynamics and may result in the formation of a new ramp. However there are no observations to support this alternative scenario for shock front nonstationarity in particular in the shock observed by Cluster and studied here.

Conclusions

1.Short separation between two Cluster spacecraft enabled direct observation of the shock front nonstationarity process.

2. Data presented show evidence in favor of the front nonstationarity model proposed by Krasnoselskikh (1985).

3. Spatial scales of substructures assume short spatial scale electric field within the ramp that could lead to the non-adiabatic thermalization of electrons.

Balikhin, M., et al. (2005), Geophys. Res. Lett. 32(24), L24106, doi:10.1029/2005GL024660.

Comisel, H. et al. (2011), Ann. Geophys. 29, 263–274, doi:10.5194/angeo-29-263-2011.

Dimmock, A.P. et al. (2012), J. Geophys. Res. (Sp. Phys.) 117, 2210, doi:10.1029/2011JA017089.

A. A. Galeev, et al. (1988), Sov. J. Plasma Phys. 14, 697

Lobzin, V.V., et al. (2007), Geophys. Res. Lett. 34, 5107, doi:10.1029/2006GL029095.

Krasnoselskikh, V. (1985), Sov. Phys. JETP 62, 282-294.

Krasnoselskikh, V. V., et al. (2002),, Physics of Plasmas 9, 1192 (2002); doi: 10.1063/1.1457465

Krasnoselskikh, V., et al. (2013), Space Sci. Rev. 178, 535–598, doi:10.1007/s11214-013-9972-y.

Livsey, W.A., et al. (1984), J. Geophys. Res. A89, 6824.

Peredo, M. et al. (1995), J. Geophys. Res. A100, 7907-7916, doi:10.1029/94JA02545.

Quest, K. B. (1985), Phys. Rev. Lett. 54, 1872

Quest, K. B. (1986), J. Geophys. Res., Space Phys. 91, 8805

Sagdeev R. Z., (1961), In Plasma Physics and the Problem of Controlled Thermonuclear Reactions, Vol iV, 454, Eds M. A. Leontovich

Sagdeev, R. Z. (1966), in Reviews of Plasma Physics, edited by M. A. Leontovich, Consultants Bureau, New York, 1966, Vol. 4, p. 23

Vaisberg, O. et al. (1986), Adv. Space Res. 6, 41 1986.

Walker, S.N., et al (1999), Geophys. Res. Lett. 26(10), 1357-1360, doi:10.1029/1999GL900210.

Woods, L.C. (1969), J. Plasma Phys.,2,435.